Effective volume of voids for flux pinning in superconductors

G. P. van der Meij and P. H. Kes
Kamerlingh Onnes Laboratory, University of Leiden, P.O. Box 9506, 2300-RA Leiden, The Netherlands
(Received 7 November 1983)

Flux pinning by voids in niobium and vanadium has been investigated. It is discussed how the collective pinning theory of Larkin and Ovchinnikov may be applied in the case where plastic defects mainly determine the disorder in the flux-line lattice. It is argued that the macroscopic pinning force above its maximum close to the upper critical field is described by the amorphous limit of the collective pinning theory. This provides a means for comparing the elementary interaction, deduced from experiment, with the recent nonlocal theory of Thuneberg *et al.* that predicts an appreciable enhancement of the effective void volume for pinning. Good agreement is obtained for niobium; the results of vanadium are satisfactory.

I. INTRODUCTION

Voids in the crystal lattice of a type-II superconductor form a well-defined model system for the study of the two ingredients of flux pinning, i.e., the maximum elementary interaction f_p between a flux line and a single defect, and the statistical summation of all the elementary interactions in a unit volume yielding the experimental pinning-force density (volume pinning force) F_p. Very recently, Thuneberg *et al.*[1] demonstrated that the semimicroscopic treatment of the quasiparticle scattering by voids of diameter D, small compared to the BCS coherence length ξ_0, gives an enhancement of the elementary interaction by a factor $\approx\xi_0/D$, that is, the volume of the pinning center is replaced by an effective volume $V_{\rm eff}\approx D^2\xi_0$. This theory is only valid for pure superconductors with an electronic mean free path $l>\xi_0$. It is also limited to the case of low flux densities, $B<0.2\mu_0 H_{c2}$, where the flux lines are well separated.[2] Of much more practical importance is the range of inductions closer to the upper critical field $\mu_0 H_{c2}$. In Sec. II A we propose an extension of a still unpublished result of Thuneberg[3] valid for $T\lesssim T_c$ and $B\lesssim\mu_0 H_{c2}$ to the regime $b=B/\mu_0 H_{c2}>0.5$ for all temperatures $T<T_c$. In an appendix we present a simple picture that illustrates the microscopic origin of the effective volume enhancement.

The aim of this work is to provide experimental evidence for the Thuneberg theory. A serious problem arises since no consensus exists as yet about the appropriate theory of summation. For systems of randomly distributed small point pins [$D<\xi(T)$ with $\xi(T)$ the Ginzburg-Landau coherence length], the commonly used summation theories[4] are only valid for independently acting pins (dilute limit). Because of the independency and the randomness, the net volume pinning force is always zero, except if the pins are strong enough to produce elastic instabilities in the flux-line lattice (FLL). This occurs if f_p exceeds a value required by the threshold criterion.[4,5] Kramer[5] showed that even for voids as large as 40 nm the threshold criterion is not fulfilled except very close to H_{c2}. Nevertheless, strong pinning is observed at all fields. The enhancement of f_p (Ref. 1) does not remove this discrepancy, as can be easily checked.

A second inconsistency is the nondiluteness of nearly all real pinning systems. A rough criterion for diluteness as given by Campbell and Evetts[6] is $n_v a_0^3<10^{-3}$, where n_v is the number density of pinning centers. For $B=0.2$ T one obtains $n_v<10^{18}$ m^3, whereas $n_v\gtrsim 10^{21}$ m^3 is encountered in practice.[5] Hence, in real point pin systems the pins do not act independently, but *collectively*. Larkin[7] showed that the long-range positional order in an infinitely large FLL is destroyed by collectively interacting pins, however weak the interaction. Short-range order persists in correlated regions with dimensions given by the transverse and longitudinal correlation lengths R_c and L_c, perpendicular to and parallel, respectively, with the applied field. Assuming that these correlated regions are elastically independent, Larkin and Ovchinnikov[8] (LO) obtained, using a simple statistical argument,

$$F_p=[W(0)/V_c]^{1/2}\,, \tag{1}$$

where

$$W(0)=n_v\langle f^2\rangle\approx\tfrac{1}{2}n_v f_p^2\,. \tag{2}$$

The average of the actual elementary interaction f is taken over a lattice cell. The correlated volume $V_c\approx R_c^2 L_c$ can be computed from the relations for R_c and L_c, Eqs. (50) and (51) of Ref. 8. It should be pointed out that these expressions for R_c and L_c are derived for elastic distortions only. Applying this theory to pinning by voids leads, as we will show later, to very large values for R_c and L_c and a value of F_p many orders of magnitude smaller than experimentally observed. The first positive experimental evidence for collective pinning in two dimensions[9] has been further justified very recently by Brandt[10] in extensive computer simulations. The conclusion that Eq. (1) is also valid for an amorphous FLL (Ref. 10) and therefore probably for a plastically deformed, highly disordered FLL containing many flux-line dislocations (FLD's) or other defects as well, is very important. In Ref. 10 it is also concluded that an amorphous FLL in the *absence* of pinning centers is not stable and relaxes back to a perfect

FLL; the presence of pinning centers, however, seem to stabilize the amorphous structure, at least within practical relaxation times.

The correlation lengths in a FLL with defects cannot be computed from the LO expressions, so that the correlated volume must be considered as an experimental parameter which probes the amount of disorder in the FLL. In a very recent paper Kerchner[11] adapted this view, but also argued that a correlated region (flux bundle) should contain at least a few hundred flux lines in order that the shear strength of the FLL is not exceeded within the correlated region. This constraint would qualitatively explain the frequently observed linear decrease of F_p at fields just below H_{c2}, but the quantitative agreement is still not satisfactory. As we will discuss in Sec. II B there are good reasons to relax Kerchner's constraint and to allow much smaller correlation lengths R_c related with the existence of a very dense system of FLD's. We think that the linear decrease of F_p below H_{c2} demonstrates that R_c has obtained its smallest possible value ($R_c \approx a_0$), so that the FLL must be considered to be amorphous.[9]

After the description of the sample preparation (Sec. III A) and experimental procedures (Sec. III B), the experimental results are presented (Sec. IV) and discussed (Sec. V). In this paper we concentrate the discussion on the results close to H_{c2} because, assuming the amorphousness of the FLL, only in this region we are able to compare our data with the extension of the Thuneberg expression for f_p [Eq. (3c)]. The agreement is very reasonable both for our Nb and V samples. For a more extensive discussion, especially on the ac-pinning behavior, we refer to Ref. 12 and a planned forthcoming paper.

II. CONSIDERATIONS ON THE THEORIES APPLIED

A. Elementary interaction of a void

Very recently, Thuneberg[3] derived the maximum elementary pinning force of a void for the case of overlapping vortices close to the upper critical field $\mu_0 H_{c2}$ in the Ginzburg-Landau regime, $T_c - T \ll T_c$. For $D \ll \xi_0$ and $l \gg \xi_0$ he obtains

$$f_p = 4.36 \frac{k_B T_c}{\xi(T=0)} \frac{k_F^2 \sigma_{tr}}{4\pi} \frac{2\kappa^2(1-b)}{1+\beta_A(2\kappa^2-1)} (1-t)^{5/2} , \quad (3a)$$

with k_F the Fermi wave vector, σ_{tr} the transport cross section of the void [we will henceforth assume $\sigma_{tr} = (\pi/4)D^2$ for the spherical voids in our samples], $\xi(0) = 0.74\xi_0$, κ the Ginzburg-Landau parameter, $\beta_A = 1.16$ for the triangular FLL, and $t = T/T_c$. The factor $1-b$ expresses the fact that the pinning energy is proportional to the average squared order parameter $\langle |\psi|^2 \rangle$.

With the use of well-known BCS expressions,[13] valid for $T \approx T_c$, Eq. (3a) can be written as

$$f_p = 0.322 \left[\frac{2\pi}{a_0(1)} \right]^3 \xi^2(T) \mu_0 H_c^2(T) \times \frac{2\kappa^2(1-b)}{1+\beta_A(2\kappa^2-1)} \sigma_{tr} \xi_0 . \quad (3b)$$

Here $a_0(1)$ denotes the FLL parameter at $b=1$, and $\xi(T) = (\Phi_0/2\pi\mu_0 H_{c2})^{1/2}$ denotes the Ginzburg-Landau coherence length. In this form Eq. (3b) can be compared to the result of the local theory for f_p derived independently by Kramer[5] and Fähnle,[14] based on the expression for the free-energy density given by Campbell and Evetts.[6] For $b \approx 1$ we note the replacement of the actual void volume by an effective volume $0.73\sigma_{tr}\xi_0$. In practice, experiments are carried out at temperatures far below T_c and in a much larger field range. In absence of a microscopic theory, we propose the following extension of Eq. (3b) as a reasonable estimate of f_p at all temperatures and inductions $B \gtrsim 0.5\mu_0 H_{c2}$:

$$f_p = 0.322 \left[\frac{2\pi}{a_0(b)} \right]^3 \xi^2(T) \mu_0 H_c^2(T) \langle |\psi|^2 \rangle \sigma_{tr} \xi_0 . \quad (3c)$$

Here, $a_0(b) = (2\Phi_0/\sqrt{3}\mu_0 H_{c2} b)^{1/2}$ and $\langle |\psi|^2 \rangle$ for weak coupling pure superconductors is given by[15]

$$\langle |\psi|^2 \rangle_{pure} = \frac{2H_{c2}(T) \left[H_{c2}(T) - \frac{T}{2} \frac{dH_{c2}}{dT} \right]}{H_c^2(0) \left[\frac{\Delta(T)}{\Delta(0)} \right]^2} \times \frac{1-b}{1+\beta_A[2\kappa_2^2(T)-1]} . \quad (4)$$

The energy gap $\Delta(T)$ is tabulated by Mühlschlegel.[16] For $T \to T_c$, Eq. (4) yields the κ factor in Eq. (3b), whereas for $T=0$ the result is $4\kappa_1^2(0)/\{1+\beta_A[2\kappa_2^2(0)-1]\}$. The Maki parameters $\kappa_1(T)$ and $\kappa_2(T)$ were defined as in Ref. 17. The factor $(2\pi/a_0)^3$ in f_p was explicitly retained since the theoretical expression[18] for the pinning energy is proportional to $|\text{grad}\psi|^2$.[17] It turns out that the temperature dependence of $\langle |\psi|^2 \rangle$ is important for the relatively pure, low-κ materials of our experiments (vanadium and niobium). Equations (3c) and (4) were used to compute the elementary pinning force for small voids.

B. Summation problem

Elastic instabilities in the FLL also occur when the shear strength σ_c of the FLL is exceeded locally.[19] It is well known that dislocations reduce the shear strength of crystal considerably,[20] and the same is likely to be true for edge FLD's. To clarify our ideas we first consider a two-dimensional FLL. FLD's enable the flux lines to adapt better to the random distribution of pins.[5] Effectively, the elastic moduli are reduced; the FLL becomes softer. When the FLL is moved past the pinning centers new FLD's may be generated. Equilibrium is obtained when the sum of the shear stresses due to the pins and due to the strain field of the FLD's nowhwere exceeds σ_c. Even without forming grain boundaries, a distribution of FLD's disturbs the positional order of the FLL since the positions of flux lines close to an FLD on opposite sides of the glide plane are uncorrelated. If we assume a density of FLD's n_d and a width w ($w \sim a_0$),[20] we may estimate the correlation length R_{cd} due to FLD's from $R_{cd} \sim (w n_d)^{-1}$. It follows that a high dislocation density reduces the correlated regions and therefore enhances the volume pin-

ning force due to Eq. (1). This stabilizes the disorder in the FLL. Of course, the energy of this metastable state is higher than that for the LO structure. In this picture there is no constraint on the minimum bundle size[11] other than $R_{cd} \sim a_0$, which defines an amorphous FLL structure indistinguishable from a very high dislocation density.[21]

Indirect evidence for FLD's is the observation of history effects[22,23] which also occur in our experiments.[12] But the work of Essmann and Träuble[24] irrefutably shows the existence of FLD's in a highly disordered and even amorphous FLL at low flux densities. The reason is that the difference in free energy of an FLL with a square or triangular symmetry is only 2%, so that both the shear modulus c_{66}, and the line energy of an edge FLD are very small.[25–27] Screw dislocations may also occur,[26] although these are not observable. Their line energy is larger[27] by a factor $(c_{44}/c_{66})^{1/2}$, where c_{44} is the tilt modulus ($c_{44} \gg c_{66}$). Screw dislocations are not stable because they can glide along the field direction, but they are probably stabilized by the pinning centers. At intermediate flux densities the FLL becomes stiffer and more ordered, but still with a very high (edge) dislocation density (some orders of magnitude more than in strongly deformed metals).[24] Close to H_{c2} direct observation of the FLL is not possible. However, it is known that the shear modulus goes to zero proportional to $(1-b)^2$, and it is also known that the FLL becomes much more susceptible for shear and tilt distortions of short wavelengths ($\approx 2\pi/k_B \approx a_0\sqrt{\pi}$), so that the effective tilt modulus for $b \to 1$ becomes[25,8]

$$\tilde{c}_{44} \approx c_{44}(1+k_B^2/k_h^2)^{-1} \approx c_{44}(1-b)/\kappa^2 . \quad (5)$$

Here $k_B^2 \equiv 2b/\xi^2$ gives the radius of the first Brillouin zone in the reciprocal FLL, and

$$k_h^2 = \frac{\langle |\psi|^2 \rangle}{\lambda^2} \approx \frac{2\kappa^2}{1+\beta_A(2\kappa^2-1)} \frac{1-b}{\lambda^2} , \quad (6)$$

with λ the magnetic penetration depth, defines the magnetic interaction range in the FLL close to H_{c2}.[25] Since the elementary interaction varies proportional to $1-b$, the increasing softness of the FLL leads to larger distortions, especially of the shear. The disorder in the FLL therefore increases, and close to H_{c2} it is expected that the FLL becomes amorphous again.

For the transverse correlation length this means that at low flux densities, $R_c \approx a_0$. With increasing field R_c rises, depending on the strength of the pins, to a maximum value. In still higher fields R_c decreases until it reaches a_0 again close to H_{c2} in a way resembling the behavior found for two-dimensional collective pinning.[9] At the field b_p where $R_c \approx a_0$, F_p attains its maximum (peak) value. For $b_p < b < 1$, F_p decreases almost linearly with $1-b$. The longitudinal correlation length L_c depends on the density of screw FLD's as well as on the disorder in the plane perpendicular to the field. Both L_c/R_c, as given by the LO theory, and the ratio of the line energy of a screw and an edge FLD, have the same field dependence, i.e., approximately proportional to $(c_{44}/c_{66})^{1/2}$ far from H_{c2}, and proportional to $(\tilde{c}_{44}/c_{66})^{1/2}$ closer to H_{c2}. Therefore it seems reasonable to estimate L_c below the peak from this factor as well as the value of R_c which may be determined from Eq. (1) supposing $W(0)$ is known.

In the amorphous limit, the LO theory predicts [Eq. (57) of Ref. 8]

$$L_c = \left[\frac{\pi B^4 k_h^4 a_0^6 r_f^2}{\mu_0^2 W(0)} \right]^{1/3} , \quad (7)$$

where r_f is the range of the pinning potential, i.e., close to H_{c2}, $r_f \approx a_0/2$ (Ref. 9) [for isolated flux lines, it might be $r_f \approx \xi$ (Ref. 10)]. From Eq. (7) it is seen that L_c is constant for $b \lesssim 1$, reflecting that (i) the correlation lengths no longer explicitly depend on c_{66}, and (ii) that

$$B^4 k_h^4 a_0^4/\mu_0^2 W(0) \propto (\tilde{c}_{44}/f_p)^2$$

is constant here. Hence the disorder in the field direction has also become independent of field. The FLL has adjusted itself optimally to the configuration of the pins. The same still holds if L_c is not purely determined by Eq. (7), but also depends on the amount of screw FLD's that might be frozen in. Therefore, Eq. (7) should be considered as an upper bound for L_c in the case $R_c \approx a_0$. Whether Eq. (7) applies to experiments or not depends on the way the experiments are carried out, as will be discussed in Sec. IV B. The volume pinning force is given by

$$F_p = \left[\frac{\mu_0 W^2(0)}{\pi^{1/2} B^2 k_h^2 a_0^6 r_f} \right]^{1/3} . \quad (8)$$

It has to be realized that all the expressions of the LO theory are only accurate up to a numerical factor of the order 1. It is interesting to note that in some practical cases the amorphous limit leads to macroscopic pinning forces approaching the direct summation limit[5,10] $F_p^d = n_v f_p$. For instance, inserting some reasonable numbers $R_c = a_0$, $L_c = 50a_0$, $a_0 = 10^{-7}$ m, and $n_v = 10^{21}$ m^{-3} in Eq. (1) yields $F_p = 0.1 F_p^d$. As one can easily check on the field dependence of Eq. (8), this result holds reasonably well for all fields $b \gtrsim 0.5$. It probably indicates that in many experimental cases where the direct summation law seems to be observed, one should instead think of a highly disordered or amorphous FLL.

III. EXPERIMENTAL

A. Samples

Rectangular niobium samples were prepared from Marz-Grade foils. One set of foils was annealed and degassed for 45 min at 2100 °C by means of Joule heating in a vacuum of 3×10^{-6} Pa. Another set was annealed in a vacuum better than 10^{-6} Pa for 4 h at 1300 °C. The samples cut from these foils are referred to as Nb-I and Nb-II, respectively. Their sizes are typically $20 \times 3 \times 0.2$ or $20 \times 3 \times 0.06$ mm^3. They all were electropolished, revealing grain sizes of about 1 mm. The residual resistance ratios of Nb-I is about 450 and that of Nb-II is about 50, which indicates a larger content of oxygen and/or nitrogen in the latter.[28] More details about the procedures are given in Ref. 29.

Neutron irradiations were carried out in the high-flux reactor of the Netherlands Energy Research Foundation

in Petten, The Netherlands. The fast-neutron dose ($E>1$ MeV) was 4.4×10^{24}m^{-2} in a 24-d irradiation cycle at temperatures between 550 and 1000 °C, at which voids are created by vacancy clustering. Other irradiation defects anneal out at these temperatures except for a fraction of the dislocation loops, but the loops' number density is about 2 orders of magnitude less than that of the voids. The number density and size distributions were obtained by transmission electron microscopy on the same samples that were selected for the flux-pinning measurements. The samples are labeled by an additional symbol *N*, *S*, *M*, and *L* referring to no voids (not irradiated), small voids, medium voids, and large voids, respectively. Some relevant data are given in Table I. The data for n_v and $D=\langle D^3\rangle^{1/3}$ are average values determined from the size distributions with a full width at half maximum denoted by ΔD (See Ref. 12 for more details). The preparation of the vanadium samples (foils of $15\times4\times0.2$ mm^3) has been discussed in a previous paper.[30] The data are also listed in Table I.

In order to suppress flux pinning by the surface all specimens were heated in an oxygen atmosphere: niobium for 10 min at 330 °C, and vanadium for 3 min at 460 °C. This treatment produces an oxygen diffusion profile at the surface with an average effective thickness of ≈0.7 and ≈4 μm, for niobium and vanadium, respectively, which reduces the surface pinning appreciably.[29]

B. Experimental procedures

All specimens were mounted in evacuated glass tubes (10^{-3} Pa at room temperature) that were painted black to avoid heating by radiation. The sample was glued to a copper foil on which a manganin heater was mounted close to the top of the sample, as well as a carbon resistor and a small reference sample of Nb, both at a distance of 4 cm below the sample. In this way the temperature could be easily raised above T_c, and the reference sample provided a fixed calibration point at T_c(Nb-I-*N*)=9.277 K.[31] The two copper leads (0.3 mm in diameter and 5 cm long) to the heater established the thermal contact with the ^{4}He bath. A 0.1-mm manganin wire acted both as a support and as an electrical lead to the carbon thermometer. The latter provided temperature readings with an accuracy better than 5 mK using an interpolation formula[32] between the fixed point and the calibration data below 4.20 K. An electronic temperature controller kept the temperature constant within 3 mK. The glass tube fitted closely in a compensated-coil system that was used for measurements both in a ramped field and a dc plus superimposed sinusoidal ac field, $H=H_{dc}+H_{ac}\cos(\omega t)$, with $H_{ac}\ll H_{dc}$.

We measured the dc magnetization at several temperatures between 1.1 K and T_c by integration of the signal from the coil system. From the irreversible magnetization curves in increasing and decreasing field, the volume pinning force and the reversible magnetization curve can be determined by an iterative procedure,[33] if H_{c1} and H_{c2} are known. For the Nb samples this procedure could be readily applied, but for the V samples H_{c1} could not be determined experimentally, so we used a comparison with theory as described in Ref. 30. At roughly the same temperatures, ac measurements were carried out as well, utilizing several techniques in order to determine the fundamental permeability[34] (μ',μ''), the flat-mode permeability[35] (μ_F',μ_F''), and the $B(H)$ hysteresis loops.[36] The flat-mode signal μ_F' is proportional to the difference in the average flux density in maximum and minimum field ($H=H_{dc}\pm H_{ac}$). An extension[12] of the uniform pinning model of Campbell[37] enabled us to determine $F(u)$ loops from the measured hysteresis loops. Here F is the macroscopic driving force (proportional to the flux density gradient) and u is the average displacement of the FLL, both determined at the surface. Most experiments were carried out at 27 Hz for several amplitudes (typically $\mu_0H_{ac}=4$ mT). A small frequency dependence of μ' was detected, which is caused by the magnetocaloric effect related to the periodic creation and annihilation of flux lines, also leading to temperature oscillations of a few mK with the fundamental frequency. In the measurements of the hysteresis loops this effect shows up as a phase shift of about 1°. At 1.1 Hz the thermal contact with the He bath is suf-

TABLE I. Characteristics of unirradiated and irradiated niobium and vanadium samples.

Sample	Nb-I-*N*	Nb-I-*S*	Nb-I-*L*	Nb-II-*N*	Nb-II-*S*	Nb-II-*L*	V-*N*	V-*S*	V-*M*	V-*L*
T_{irr} (°C)		>500	>640		>500	>640		450	535	590
n_v (10^{21} m^{-3})		9.6	1.8		15	2.3		4.8	0.65	0.09
D (nm)		3.6	7.0		3.5	7.5		4.5	18	27
ΔD (nm)		1.0	2.5		1.0	5.5		1.5	15	20
$\rho_{293\,K}/\rho_{4.2\,K}$	390	150[a]	380[a]	50	40[a]	28[a]	310	220	57	106
T_c (K)	9.28	9.27	9.28	9.21	9.19	9.17	5.42	5.40	5.22	5.36
ΔT_c (mK)	3	17	10	7	24	36	3	15	13	25
μ_0H_c (mT)[b]	156	159	159	152	157	155	54	51	44	50
μ_0H_{c2} (mT)[b]	272	284	278	313	326	344	76	77	79	82
κ	0.78	0.83	0.78	0.96	1.01	1.10	0.85	0.98	1.15	1.05
$\rho_{4.2\,K}$ (nΩ m)	0.37	1.1[a]	0.37[a]	2.9	3.4[a]	3.9[a]	0.64	0.90	3.5	1.9
l (nm)	840	320[a]	830[a]	110	90[a]	60[a]	550	390	100	180
ρ_D[c]	0.04	0.1[a]	0.05[a]	0.3	0.4[a]	0.6[a]	0.07	0.1	0.4	0.2

[a]Data obtained from κ and κ_0 using Gorkov's theory.
[b]Data at $T=4.20$ K.
[c]$\rho_D=0.882\xi_0/l$, $\xi_0=39$ nm for Nb (Ref. 40), and $\xi_0=46$ nm for V (Ref. 41).

ficiently good to give almost isothermal conditions, but the signal-to-noise ratio is poor. It was observed that the transition from the isothermal to the adiabatic limit took place at ~ 15 Hz. Therefore the experiments we are reporting on here were done at 27 Hz, which is close to adiabatic. In this case it is possible to correct for the effect using elementary thermodynamics, as is discussed extensively in Ref. 12. Upon comparison with measurements at 1.1 Hz, the correction is found to be somewhat too large (up to a factor of 1.5), but we consider this to be of minor importance since the effect itself is at most 15%.

It is essential to define the starting conditions of the ac measurements. If the dc field is applied first, and then subsequently the ac field is applied, then the critical state is the starting condition. If, after applying the ac field, it is raised sufficiently (20 mT) as to erase the memory by shaking the flux lines over many lattice parameters before gradually decreasing the amplitude to the measuring value, then the starting condition is called the homogeneous state. Thus, because it was observed that, irrespective of the history, the latter procedure causes the magnetization to attain its reversible value indicating a homogeneous flux distribution. Therefore the procedure is refered to as homogenization (note the analogy with the demagnetization of ferromagnets).

IV. RESULTS

A. General properties

The critical temperatures and transition widths ΔT_c were determined from permeability measurements in zero applied dc field and a 0.1-mT ac field. They are listed in Table I together with the values of $\mu_0 H_{c2}$ and $\mu_0 H_c$ determined from the magnetization curves at 4.20 K. From the slope of the computed reversible magnetization curve, κ_2 was obtained, and from $\kappa_2(t)$, the value of $\kappa=\kappa_2(1)$ was obtained. The resistivity at 4.2 K for the irradiated niobium samples was not measured directly for safety reasons and was therefore obtained from κ by means of Gorkov's theoretical expression[38] and the value of $\kappa_0=0.77$ for pure niobium.[39] The resistance ratio $\rho_{293\,\mathrm{K}}/\rho_{4.2\,\mathrm{K}}$, the mean free path of the electrons l, and the dirt parameter $\rho_D=0.882\xi_0/l$ were determined from $\rho_{4.2\,\mathrm{K}}$ and are also given in the table. We used $\xi_0=39$ nm for niobium[40] and $\xi_0=46$ nm for vanadium.[41]

The results of $\kappa_1(t)/\kappa$ and $\kappa_2(t)/\kappa$ compare well with those of other data known in the literature (see Refs. 39 and 41). The effect of the different heat treatments of the niobium samples is clearly reflected in the systematic differences in T_c, $\mu_0 H_{c2}(4.2\,\mathrm{K})$, and $\rho_{4.2\,\mathrm{K}}$. These results agree very well with the observations of Koch *et al.*,[42] who studied the influence of oxygen on the properties of Nb. We concluded for an oxygen content of 65 and 580 at. ppm for Nb-I-*N* and Nb-II-*N*, respectively. In spite of many precautions it turned out that after the irradiation these values were increased with 10—70 at. ppm for the Nb-I and with 100—200 at. ppm for the Nb-II samples. The origin of this contamination is not yet clear.

The vanadium samples also show a decrease of T_c after the irradiation. Though oxygen reduces the T_c of vanadium,[41] we think this time that the effect is caused by the conversion of ^{51}V into ^{52}Cr after the capture of thermal neutrons and β decay. de Sorbo[43] reported a decrease of T_c of 0.3 K/at.% for a solid solution of Cr in V. A thermal neutron dose of 15×10^{24} m^{-2} for V-*M* would lead to a Cr content of 0.7 at.% and a reduction of 200 mK. For V-*S* and V-*L*, 30 mK is estimated. Both values agree well with the measured shifts in T_c.

The transition widths $\Delta T_c \equiv dT/d\mu'$ at $\mu'=0.5$ range from 10 to 36 mK, indicating that the samples are still reasonably homogeneous after the irradiations. The same can be concluded from the rounding of the magnetization curves at H_{c2}, which leads to an uncertainty in H_{c2} that turns out to be proportional to ΔT_c and lies between 2 and 10 mT for Nb at 4.2 K.

The dirt parameter for all irradiated samples is found to be sufficiently small to assure the validity of the pure-limit approximations by Thuneberg *et al.*[1,3] and by Maki and Tsuzuki.[15]

B. Pinning properties

In Fig. 1 two representative examples of magnetization curves are shown. It is indicated how $\mu_0 H_{c1}$ and $\mu_0 H_{c2}$ were defined, and how the iterative procedure worked: The circles denote the average magnetizations, and the pluses denote the reversible magnetizations obtained in the next iteration step. The dashed line represents a fit[12] to the reversible data from which the slope of the reversible magnetization curve could be computed. This quantity, in the form $\mu_A=(\partial B/\partial H)_{\mathrm{rev}}$, has to be known in low-κ materials in order to evaluate the dc and ac pinning data. Obviously, the experimental uncertainty in μ_A of vanadium is much larger than that of niobium. History effects, as indicated by the lines in the inset of Fig. 1(a), are clearly observed when the magnetic field ramp is inverted. These curves show that F_p is appreciably smaller upon reversal than if the field is reduced starting above H_{c2}. Since F_p depends on history effects, it might be different for the upper and lower magnetization curves at the same field. Therefore, F_p determined from the magnetization should be considered as an average value. However, the deviation of the average from the actual value is small because the reversible curve in Fig. 1 coincides well with the magnetization measured after homogenization.

In Fig. 2 the $F_p(b)$ data for all the irradiated samples at 4.20 K are shown. The behavior above the field b_p at which F_p is maximum (the peak) is quite similar for all samples. The lines represent the functional dependence of Eq. (8) adapted at $\bar{b}=(1+b_p)/2$. Scaling[19] is observed above the peak if we plot the $F_p(b)/F_p(\bar{b})$ data measured at different temperatures in one diagram. Below b_p, the results do not scale. We should note that, usually, $F_p(b)/F_p(b_p)$ data are plotted to study the scaling behavior.[19] If we do so, scaling for $b>b_p$ is only found for Nb-II-*L*, V-*S*, and V-*L*. For the other samples, b_p decreases with decreasing temperature, roughly by 10—20%. Below b_p, scaling is never observed. This behavior is expected when the pinning force below the peak depends on the density of FLD's and that above the peak is determined by the amorphousness of the FLL. At lower tem-

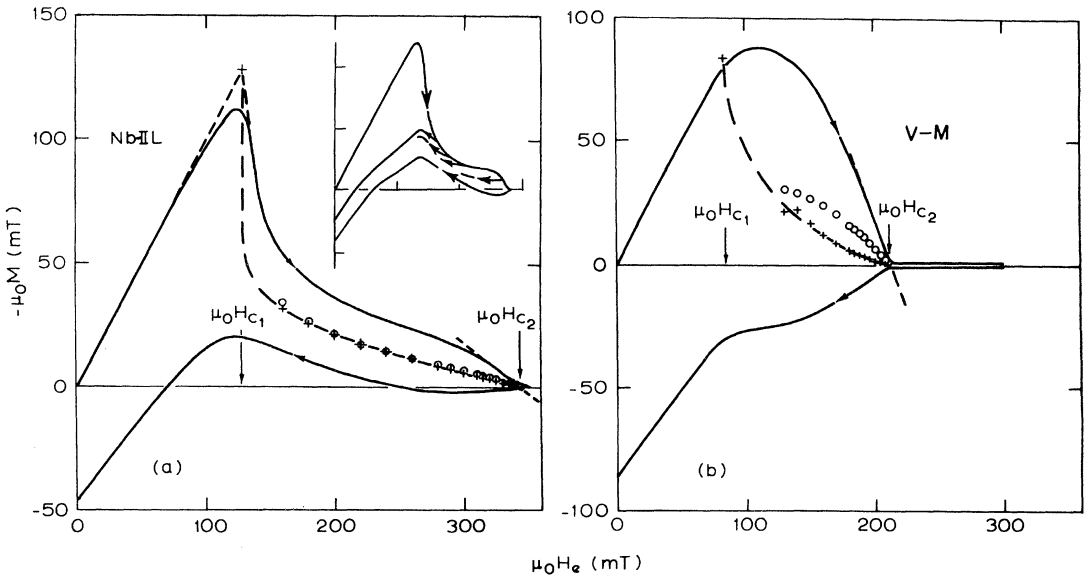

FIG. 1. Typical magnetization curves for the samples (a) Nb-II-L at 4.20 K and (b) V-M at 2.51 K. Solid curves denote experimental irreversal magnetizations in increasing and decreasing fields; the values of the lower and upper critical fields are indicated in the figures. Circles denote average magnetization. Pluses denote reversible magnetization obtained by the iteration procedure described in Ref. 33. Dashed lines denote computer fits to the reversible data. Inset of (a) shows the history effects observed after several field-ramp reversals for the sample Nb-I-L at 4.2 K.

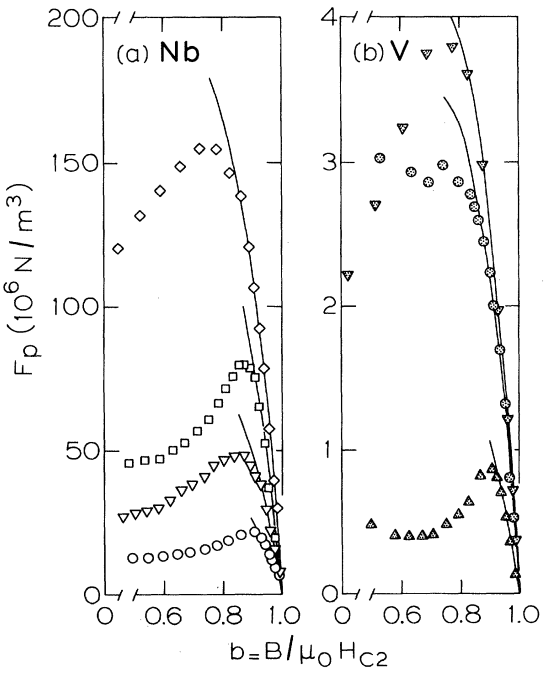

FIG. 2. Volume pinning forces vs reduced flux density at 4.20 K for (a) the niobium samples and (b) the vanadium samples. Open symbols: Nb-I-S (circles), Nb-I-L (squares), Nb-II-S (inverted triangles), and Nb-II-L (diamonds). Solid symbols: V-S (triangles), V-M (inverted triangles), and V-L (circles). The upcurve below $b \sim 0.7$ is not seen at other temperatures, and may therefore be attributed to experimental inaccuracies. The solid lines represent the field dependence of the collective pinning prediction for an amorphous FLL, Eq. (8), adapted at $\bar{b} = (1 + b_p)/2$, where b_p is the value at which F_p is maximal.

peratures the elastic distortions of the FLL are larger, so that a higher FLD density can be expected. Also as a result, a more extended amorphous regime is anticipated, in agreement with the shift of b_p with temperature.

It is worth noting that Steingart *et al.*,[22] in their study of the effect of the FLL history on the critical current in niobium, report an enhancement of I_c when the FLL was formed by cooling in a field in the presence of a transport

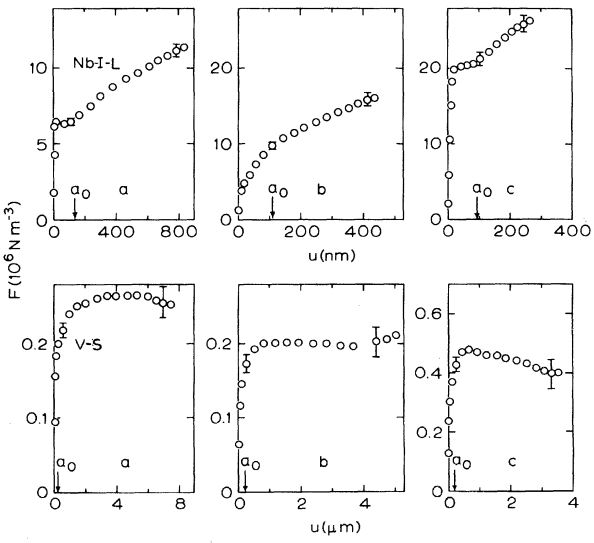

FIG. 3. Typical results of ac hysteresis loops experiments: volume driving force F vs average FLL displacement u at the surface for the samples Nb-I-L (upper three graphs) and V-S (lower three graphs), both at $T = 4.20$ K and at values of the reduced flux density $B/\mu_0 H_{c2}$ of (a) 0.5, (b) 0.75, and (c) ~ 0.93. The value of the FLL parameter a_0 is also indicated.

current. They suggest an analogy with fatigue effects in mechanical deformation. Their discussion in terms of the number of "effective" pins still applies if one thinks instead in terms of FLD density and related correlated regions. The fact that the enhancement is only observed below the sharp peak in I_c, and that it disappears above the peak, is very interesting. This suggests that above the peak the FLL is always optimally adjusted to the distribution of pins, a state we like to regard as the amorphous limit.

Another interesting analogy is that between the correlated volume and the activation volume as determined in flux creep experiments by Beasley *et al.*[44] The data reported on the product of the activation volume V and the width of the pinning barrier $X \approx a_0/2$ compare well, both as to the magnitude and to the temperature and field dependence, with the expectations for the correlated volume as mentioned in Sec. II B. Again of special importance is the observation that VX becomes constant approaching H_{c2}, and appears to have a value of $(40-100)a_0^4$, depending on the pinning strength. The fact that these analogies occur in systems with different kinds of pins (dislocations in Refs. 22 and 44, voids in this work) demonstrates that the nature of the pins is not very relevant for the interpretation in terms of very small correlated regions. We especially note that the behavior in the regime just below H_{c2} is quite general, reflecting the amorphousness of the FLL ($R_c \approx a_0$). Only the (constant) value of L_c may depend on the strength of the pins.

The ac measurements provided plots of $F(u)$ as shown for Nb-I-L and V-S in Fig. 3. These data were taken at 4.20 K and at amplitudes of 4 and 3 mT, respectively. The initial condition was the homogeneous state; corrections were made for the magnetocaloric temperature oscillations. Three typical cases are displayed, i.e., for a field far below the peak (curves labeled a at $b=0.5$), a field close to the peak (curves labeled b at $b=0.75$), and a field above the peak (curves labeled c at $b \approx 0.93$). Some general features should be mentioned. For vanadium the ac displacements of the FLL relative to the lattice parameter a_0 are much larger than for niobium. Related to this, as will be discussed later, is the saturation, within experimental accuracy, of $F(u)$ at $u \gg a_0$ for vanadium, whereas for niobium a continuous increase of the driving force with displacement is observed. When, for niobium, the ac amplitude was sufficiently large, eventually the same saturation of $F(u)$ was detected at displacements larger than $(5-10)a_0$. A closer inspection of the vanadium results in Fig. 3 actually reveals that the steep linear rise is also followed by a more gradual increase up to a saturation level.

This typical ac behavior of the FLL can be explained in the following qualitative way. We first note that the homogeneous state is a very important initial condition to facilitate observation of stable behavior. It constitutes a homogeneous flux distribution with larger sizes of the correlated regions than in the critical state, as will be argued later. The initial steep rise is attributed to the reversible displacement[35] of the correlated regions over distances smaller than $a_0/2$. Second, quite analogous to the stress-strain behavior of solids, we regard the slip of FLD's as the mechanism responsible for the subsequent, more gradual increase of $F(u)$.[12] The slip stops when the driving force is in equilibrium with the macroscopic pinning force belonging to the particular distribution of FLD's that determines the size of the correlated regions, as discussed in Sec. II B. After a displacement over one lattice parameter the driving force still appears to be much smaller than F_p determined from the dc measurements [to be denoted F_p^{dc}, whereas $F(a_0)$ will henceforth be referred to as F_p^{ac}]. This can be seen from Fig. 4 where both quantities for Nb-I-L and V-M are plotted versus b. Since the critical state is formed by a continuous compression of the FLL, it is considered as a state of optimally distributed FLD's producing the strongest pinning. A reversal of the flux movement (inset of Fig. 1) gave rise to much smaller F_p's, probably due to slip and relaxation of the stresses in the FLL. This provides the argument that the correlated regions in the homogeneous state are larger than in the corresponding critical state. Time-dependent measurements of μ_F', discussed in Ref. 12, yield even stronger evidence for this view, as well as the results of neutron scattering experiments by Thorel *et al.*[45] After increasing u over many lattice parameters, a new optimal distribution of FLD's is eventually obtained, corresponding to the level of saturation at $u \approx 10a_0$ in Fig. 3. In most cases the value of $F_p(10a_0)$ was still somewhat smaller than F_p^{dc}.

In Fig. 4 it is seen that the peak in F_p^{ac} occurs at a slightly higher field than for F_p^{dc}. The values of F_p^{ac}/F_p^{dc} below the peak are appreciably smaller than above the peak, probably because in the first case both R_c and L_c increased after the homogenization, whereas in the latter case only L_c changed, with R_c remaining at its minimum value of a_0. We expect therefore that after the homogenization procedure L_c above the peak has most closely approached its upper bound determined by the LO expression [Eq. (7)].

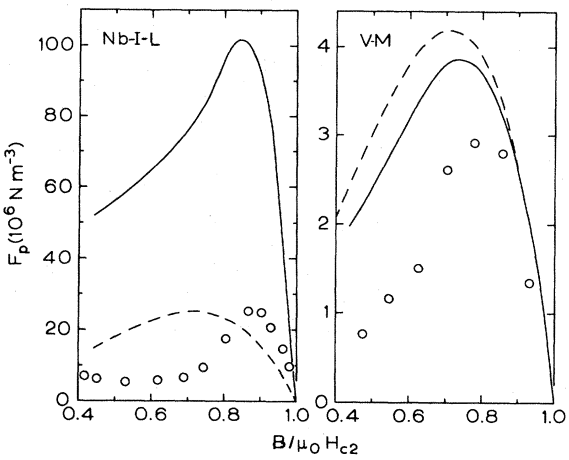

FIG. 4. Comparison of the volume pinning forces at 4.2 K for Nb-I-L (left-hand side) and V-M (right-hand side) determined from the dc-magnetization measurements (solid lines) and the ac hysteresis loops, (circles). The dahsed lines show the computed values from the collective pinning theory (Ref. 8), Eq. (8), and our *ad hoc* extension of the Thuneberg expression for the elementary pinning force (Ref. 3) Eq. (3c).

V. DISCUSSIONS AND CONCLUSIONS

A. Statistical summation

The theory of collective pinning yields unacceptable results when only elastic deformations are considered. As an example, R_c and L_c for Nb-I-L were computed from Eq. (50) of Ref. 8 as a function of field using Eq. (3c) of this paper for the elementary interaction. To summarize the results, R_c decreased continuously from 530 μm at $b=0.44$ to 4.9 μm at $b=0.97$, L_c, correspondingly, decreased continuously from 4.0 to 0.89 mm, resulting in underestimates of F_p by factors of 10^5–10^3. Apparently, theory predicts correlation lengths that are orders of magnitude too large. Consequently, the field at which, in terms of the elastic theory, the amorphous limit is attained, lies very close to H_{c2}, as does the sharp peak due to the softening of the FLL.

We think that plastic deformations cause an amorphous FLL above the peak and a highly disordered FLL below the peak. Therefore we compare the experiments displayed in Fig. 4 with the results of Eqs. (8), (2), (3c), (4), and (6) of Sec. II. For the magnetic penetration depth λ in Eq. (6) we chose the values $\lambda(0)=31.5$ nm for niobium[46,40] and $\lambda(0)=37.4$ nm for vanadium.[41] The temperature dependence of λ according to the BCS theory, tabulated in Ref. 16, was used.[46] The final results are not sensitive to the actual temperature dependence. The dashed lines in Fig. 4 show the calculations for two samples at 4.20 K. The correlation lengths and F_p can be computed by means of the relations valid for $b>0.5$,

$$R_c=C_R b^{-1/2},\quad L_c=C_L b^{-1},\quad F_p=C_F b^{5/2}(1-b)\ . \tag{9}$$

The coefficients for all the samples at 4.20 K are listed in Table II. Owing to the approximations in the collective pinning theory one may ignore discrepancies by factors of order 1.[10]

Above the peak in Fig. 4 qualitative agreement is observed for both Nb-I-L and V-M, as was expected from the coincidence of curves and data in Fig. 2. Here we see that the quantitative agreement is also satisfactory, especially for the ac experiments. For Nb-I-L at lower fields the shape of the dashed theoretical curve starts to deviate from the experimental results, indicating that the correlated regions here are roughly a factor of 4 larger than in the amorphous limit. For V-M there is no distinct change observed, indicative for a nearly constant and optimal disorder of the FLL for all fields above $b\approx 0.5$. This behavior corresponds to the "dome" shape of the $F_p(b)$ curve. In Fig. 2 such a shape is seen for the samples with the relatively largest pinning. We note a correlation between the ratio C_L/C_R given in Table II and the maximum pinning force, and also one between C_L/C_R and the shape of the curves in Fig. 2. When $C_L/C_R<100$, a dome shape is observed, whereas a more pronounced peak occurs for values above 100. Since this analysis is not based on numerous materials with different characteristics, we hesitate to stress the value of C_L/C_R as a figure of merit. However, for two reasons it seems to be a useful quantity: (i) It gives an impression of the FLL structure, and (ii) it provides a better way of comparing the disorder in the FLL in different materials caused by an identical system of pinning centers. Neither the macroscopic pinning force nor $W(0)$ are the appropriate quantities, since they are very sensitive to the superconducting properties of the material, such as $H_c(0)$ and κ. To elucidate this point in the case of voids, we compare C_L/C_R and F_p of Nb and V at 4.2 K, assuming n_v and D to be equal in both materials. In the Landau-Ginzburg regime we have

$$C_L/C_R\sim(n_v D^4\xi_0^2 H_{c2}^{3/2})^{-1/3}$$

and

$$F_p\sim(n_v D^4\xi_0^2 H_c^3 H_{c2}^{9/4})^{2/3}\ .$$

Therefore, C_L/C_R for Nb is smaller by only a factor of 0.6 whereas F_p is larger by as much as a factor of 100 (the latter in agreement with the experimental results given in Fig. 2). Thus the correlated volumes, expressed in units of a_0^3, are almost equal in both materials. This is more relevant for the strength of the pinning than the actual value of F_p.

B. Elementary pinning force

In this section we invert the procedure used above and compute the maximum elementary pinning interaction from Eqs. (8), (6), and (2), inserting the experimental values of n_v and F_p determined at the field $(1+b_p)/2$. This yields $f_p^{\rm expt}$, which is compared to $f_p^{\rm theor}$ obtained from Eqs. (3c) and (4), and the transport cross section of the voids $\pi D^2/4$. The ratios $f_p^{\rm expt}/f_p^{\rm theor}$ are plotted in Fig. 5 for all the samples versus temperature. Both $F_p^{\rm dc}$ and $F_p^{\rm ac}(a_0)$ data have been used, giving the points denoted by the open and solid symbols, respectively. As has been discussed, we expect the latter to be more reliable, but the differences turn out to be not so dramatic: Only in the case of Nb, the difference is approximately a factor of 2. The experimental error is reasonably represented by the scattering of the data for each sample.

By plotting the results versus temperature, we believe we have a more sensible and sensitive test of the applied theories than if we compared the functional dependence of F_p as in Fig. 4. Regarding the many temperature-

TABLE II. Coefficients of Eq. (9) for R_c, L_c, and F_p at $T=4.20$ K for all the samples with voids.

Sample	Nb-I-S	Nb-I-L	Nb-II-S	Nb-II-L	V-S	V-M	V-L
C_R (10^{-8} m)	9.2	9.3	8.5	8.3	18	18	17
C_L (10^{-5} m)	1.4	1.1	1.2	0.83	4.0	1.2	1.4
C_F (10^7 N m^{-3})	12	21	19	44	0.32	3.4	2.7
C_L/C_R	150	120	140	100	230	70	82

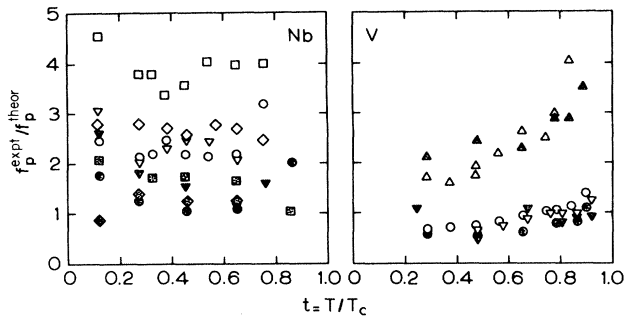

FIG. 5. Ratio of f_p^{expt} obtained from the experimental volume pinning force and Eq. (8), and f_p^{theor} computed from the nonlocal theory [Eq. (3c)], both determined at $\bar{b}=(1+b_p)/2$, plotted vs reduced temperature for all irradiated niobium (left-hand side) and vanadium samples (right-hand side). Open symbols denote dc experiments, and dark symbols denote ac measurements. Niobium samples: Nb-I-*S* (circles); Nb-I-*L* (squares); Nb-II-*S* (inverted triangles); Nb-II-*L* (diamonds). Vanadium samples: V-*S* (triangles); V-*M* (inverted triangles); V-*L* (circles).

dependent quantities that play a role in the determination of f_p^{expt}/f_p^{theor}, the nearly constant value of this ratio for niobium in Fig. 5 is striking. For the vanadium samples a slight increase with temperature is observed, which may be due to the much larger inaccuracy in the determination of the reversible properties (Sec. III A, Ref. 33), especially $\mu_0 H_c(T)$ and $(dB/dH)_{H_{c2}}$. A comparison with the parabolic law indicates that $\mu_0 H_c$ at the lower temperatures is too large ($\sim 10\%$), and consequently that $(dB/dH)_{H_{c2}}$ is too large as well, leading to f_p^{theor} being too large and f_p^{expt} being too small. This accounts for at least part of the upturn and tells us that the vanadium data at the lower temperatures are somewhat too small.

Both the niobium and vanadium results give a value for f_p^{expt}/f_p^{theor} of the order of 2. Again, the niobium data are more consistent. Mutual differences can be accounted for by the experimental error in n_v and D, which is responsible for a $\sim 40\%$ error in the final results. For the V-*M* and V-*L* samples this error may be larger since the size distribution is comparitively wide ($\Delta D/D \sim 1$) as well. A reason for the lower values of f_p^{expt}/f_p^{theor} for V-*M* and V-*L* may be the large void size ($D \sim 0.5\xi_0$), which reduces the effect of the nonlocal enhancement in Thuneberg's theory.

In view of the approximations of the summation theory, the final result $f_p^{expt}/f_p^{theor} \approx 2$ is quite reasonable. On the other hand, it leaves an uncertainty as to the numerical accuracy of Thuneberg's expression for the elementary interaction.

C. Conclusions

For the dense random distribution of voids in our samples, flux pinning is a collective effect for which no threshold criterion applies. The LO summation theory[8] predicts very small volume pinning forces because only elastic distortions of the FLL determine the correlation lengths. Structural defects in the FLL, especially dislocations, may reduce the size of the correlated regions considerably, ultimately down to $R_c \approx a_0$, in contrast to the constraint suggested in Ref. 11. The amorphous limit of the collective pinning theory[8] describes the nearly linear decrease of F_p above the peak close to H_{c2}. If Eq. (3c) is used for the elementary pinning force, the computed F_p's agree reasonably well with the experimental results above the peak. The best agreement is obtained for our ac measurements because of the homogenization procedure. A dome-shaped $F_p(B)$ curve indicates an amorphous FLL,[9] whereas a sharp peak denotes an increase of the correlated regions below the peak field. In our samples a large amount of disorder is always present in the FLL.

Assuming the amorphousness of the FLL above the peak we were able to compare the theoretical and experimental values of the elementary pinning force. Their ratio turns out to be essentially temperature independent and of order 1. This provides the first experimental evidence for the predicted nonlocal enhancement by a factor $\sim \xi_0/D$ for the elementary pinning force of small voids.[1,3]

ACKNOWLEDGMENTS

A grant from the Netherlands Energy Research Foundation (ECN) in Petten is gratefully acknowledged. We also thank J. Bressers of the Joint Research Center EURATOM, Petten, for supplying the vanadium samples, E. V. Thuneberg and D. Rainer for correspondence and discussions concerning the elementary interaction and reporting as yet unpublished results to us, and E. H. Brandt for many stimulating discussions on the statistical summation theory and for communicating his results prior to publication. One of us (G.P.M.) would like to acknowledge the interesting discussions with A. M. Campbell, J. E. Evetts, and M. V. McLean during his visit at Cambridge University, United Kingdom.

APPENDIX

A model is introduced to illustrate the theory of Thuneberg *et al.*,[1] providing a simple picture for the microscopic mechanism involved. For a second-order transition the gap equation can be linearized to a form given by de Gennes,[47]

$$\Delta(\vec{s}) = \int K(\vec{s}-\vec{r})\Delta(\vec{r})d\vec{r}\,, \tag{A1}$$

where $K(\vec{s}-\vec{r})$ is a kernel expressing the nonlocality of the order parameter $\Delta(\vec{r})$ over a range R ($\Delta \propto \psi$). For pure homogeneous superconductors, $R \sim \xi_0$. A cross section of the situation for a small void ($D \ll \xi_0$) at $\vec{r}_v$ is depicted in Fig. 6. The range R is indicated by the dashed line around $\vec{s}$. In the pure limit ($l \gg \xi_0$) the quasiparticles travel along straight trajectories.[47,48] Scattering by the void therefore excludes the shaded area from contributing to the order parameter in $\vec{s}$. If the order parameter is homogeneous this loss is compensated for by backscattering of quasiparticles from the side of the void facing $\vec{s}$.[18] This leads only to a small change in the superconducting properties,[1] in agreement with Anderson's theorem and a remark in Ref. 47 (p. 220) that the density correlation function is not destroyed by a collision. However, if the

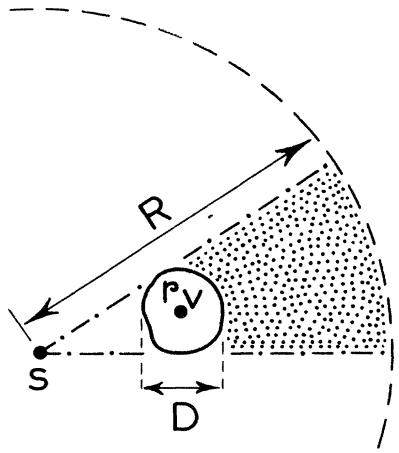

FIG. 6. Illustration of the nonlocal enhancement of the elementary interaction by the shadow effect of a spherical void of diameter D at a position $\vec{r}_v$. The range of the kernel in Eq. (A1) is indicated by R ($\sim\xi_0$ for pure superconductors). The shaded area does not contribute to the order parameter in $\vec{s}$, causing a nonlocal distortion in Δ around the void when it is situated at a place where Δ changes rapidly, e.g., the center of a flux line.

undisturbed order parameter changes rapidly at $\vec{r}_v$, this "shadow effect" is not compensated for (or even enhanced depending on the sign of Δ on both sides of the void), so that the order parameter changes drastically over a distance of order ξ_0 from the void.[1] This also yields the proper boundary conditions $\vec{\nabla}\,|\,\Delta(\vec{r})\,|=\vec{0}$ and the normal component of the current density $j_n=0$ at the surface of the void.[1,12]

Suppose the void is at the center of a flux line at $\vec{r}_v=\vec{0}$, where $\Delta=0$ and changes rapidly. With the use of the simple picture we just introduced it is easy to see that $|\Delta|$ is enhanced on both sides of the void, as shown in Fig. 1 of Ref. 1. Energy is therefore gained since the order parameter is not suppressed to zero in the flux-line core. On the other hand, condensation energy is lost if the void is at a site between the flux lines where $|\Delta|^2$ is at a maximum. In the former local approach,[6,5,14] it was just the loss in energy alone that was thought to be responsible for the elementary interaction.[49] Now, the gain in energy contributes as well and is even predominant if $D\ll\xi_0$.

The shadow effect clearly indicates that the condition $l\gg\xi_0$ is crucial for the enhancement. If $\sqrt{l}\ll\sqrt{\xi_0}$, a diffusion process determines the kernel of Eq. (A1),[47] so that the shadow effect is largely compensated. It also shows that for precipitates the situation is more complicated. For a dielectric inclusion we expect an enhancement of the effective volume. For a metallic particle the ratio of the electron mean free path and the dimensions of the precipitate will be of importance. In addition, the proximity effect must be taken into account.[50,49] The situation for very large particles $D\gg\xi(T)$ is more reminiscent for that of grain-boundary pinning,[50,51] so that in this case an effective volume $V_{\rm eff}\sim D^2\xi(T)$ is expected.

[1]E. V. Thuneberg, J. Kurkijärvi, and D. Rainer, Phys. Rev. Lett. 48, 1853 (1982); in *Proceedings of the Conference on Superconductivity in d- and f-Band Metals, Karlsruhe, 1982,* edited by W. Buckel and W. Weber (Kernforschungszentrum Karlsruhe, Karlsruhe, West Germany, 1982), p. 535.

[2]E. H. Brandt, Phys. Status Solidi B 51, 345 (1972).

[3]E. V. Thuneberg (private communication).

[4]R. Labusch, Crystal Lattice Defects 1, 1 (1969); R. Schmucker and E. H. Brandt, Phys. Status Solidi B 79, 479 (1977); A. M. Campbell, Philos. Mag. B 37, 149 (1978).

[5]E. J. Kramer, J. Nucl. Mater. 72, 5 (1978).

[6]A. M. Campbell and J. E. Evetts, Adv. Phys. 21, 199 (1972).

[7]A. I. Larkin, Zh. Eksp. Teor. Fiz. 58, 1466 (1970) [Sov. Phys.—JETP 31, 784 (1970)].

[8]A. I. Larkin and Yu. Ovchinnikov, Zh. Eksp. Teor. Fiz. Pis'ma Red 27, 301 (1978) [JETP Lett. 27, 280 (1978)]; J. Low Temp. Phys. 34, 409 (1978).

[9]P. H. Kes and C. C. Tsuei, Phys. Rev. Lett. 47, 1930 (1981); Phys. Rev. B 28, 5126 (1983).

[10]E. H. Brandt, Phys. Rev. Lett. 50, 1599 (1983); J. Low Temp. Phys. 53, 41 (1983); 53, 71 (1983).

[11]H. R. Kerchner, J. Low Temp. Phys. 50, 335 (1983).

[12]G. P. van der Meij, Ph.D. thesis, Unversity of Leiden, 1984.

[13]M. Tinkham, *Introduction to Superconductivity* (McGraw-Hill, New York, 1975), p. 113.

[14]M. Fähnle, Phys. Status Solidi B 83, 433 (1977).

[15]K. Maki and T. Tsuzuki, Phys. Rev. 139, A868 (1965); K. Maki, Phys. Rev. 156, 437 (1969).

[16]B. Mühlschlegel, Z. Phys. 155, 313 (1959).

[17]D. Saint-James, G. Sarma, and E. J. Thomas, *Type-II Superconductivity* (Pergamon, Oxford, U.K., 1969), p. 145.

[18]D. Rainer (private communication).

[19]E. J. Kramer, J. Appl. Phys. 44, 1360 (1973).

[20]A. H. Cottrell, *Dislocations and Plastic Flow in Crystals* (Clarendon, Oxford, U.K., 1953).

[21]R. M. J. Cotterill and L. B. Pedersen, Solid State Commun. 10, 439 (1972).

[22]M. Steingart, A. G. Putz, and E. J. Kramer, J. Appl. Phys. 44, 5580 (1973).

[23]H. Küpfer and W. Gey, Philos. Mag. 36, 859 (1977).

[24]U. Essmann and H. Träuble, Phys. Status Solidi 25, 395 (1968), 32, 337 (1969); J. Appl. Phys. 39, 4052 (1968).

[25]E. H. Brandt, J. Low Temp. Phys. 26, 709 (1977); 26, 735 (1977); and 28, 263 (1977); 28, 291 (1977).

[26]R. Labusch, Phys. Lett. 22, 9 (1966).

[27]F. R. N. Nabarro and A. T. Quintanilha, in *Dislocations in Solids,* edited by F. R. N. Nabarro (North-Holland, Amsterdam, 1980), Vol. V, p. 218.

[28]W. de Sorbo, Phys. Rev. 132, 107 (1963).

[29]G. P. van der Meij, P. H. Kes, and D. de Klerk, Physica 95B, 369 (1978).

[30]P. H. Kes, G. P. van der Meij, D. de Klerk, and J. Bressers, J. Nucl. Mater. 72, 40 (1978).

[31]M. Durieux and G. P. van der Meij, Comité Consultatif de Thermométrie, 13e Session, Sévres, 1980, Doc. 66 (unpublished).

[32]P. H. Kes, C. A. M. van der Klein, and D. de Klerk, Cryogenics 14, 16 (1974).

[33]P. H. Kes, C. A. M. van der Klein, and D. de Klerk, J. Low Temp. Phys. 10, 759 (1973).
[34]D. de Klerk and C. A. M. van der Klein, J. Low Temp. Phys. 6, 1 (1972).
[35]A. M. Campbell, J. Phys. C 2, 1492 (1969).
[36]R. W. Rollins, H. Küpfer, and W. Gey, J. Appl. Phys. 5, 5392 (1974).
[37]A. M. Campbell, Philos. Mag. 31, 1191 (1975).
[38]L. P. Gorkov, Zh. Eksp. Teor. Fiz. 37, 1407 (1959) [Sov. Phys.—JETP 10, 998 (1960)].
[39]H. R. Kerchner, D. K. Christen, and S. T. Sekula, Phys. Rev. B 21, 86 (1980).
[40]J. Auer and H. Ullmaier, Phys. Rev. B 7, 136 (1973).
[41]E. Moser, E. Seidl, and H. W. Weber, J. Low Temp. Phys. 49, 585 (1982).
[42]C. C. Koch, J. O. Scarbrough, and D. M. Kroeger, Phys. Rev. B 9, 888 (1974).
[43]W. de Sorbo, Phys. Rev. 130, 2177 (1963).
[44]M. R. Beasley, R. Labusch, and W. W. Webb, Phys. Rev. 181, 682 (1969).
[45]P. Thorel, R. Kahn, Y. Simon, and D. Cribier, J. Phys. (Paris) 34, 447 (1973).
[46]C. Varmazis and M. Strongin, Phys. Rev. B 10, 1885 (1974).
[47]P. G. de Gennes, *Superconductivity of Metals and Alloys* (Benjamin, New York, 1966), Chap. 7.
[48]G. Bergmann, Z. Phys. 234, 70 (1970).
[49]T. Matsushita, J. Appl. Phys. 54, 281 (1983).
[50]E. J. Kramer and H. C. Freyhardt, J. Appl. Phys. 51, 4903 (1980).
[51]G. Zerweck, J. Low Temp. Phys. 42, 1 (1981).
[52]W. E. Yetter, D. A. Thomas, and E. J. Kramer, Philos. Mag. B 46, 523 (1982); W. E. Yetter, Ph.D. thesis, Cornell University, 1980.